

Isolation and Characterization of Subnuclear Compartments from *Trypanosoma brucei*

IDENTIFICATION OF A MAJOR REPETITIVE NUCLEAR LAMINA COMPONENT*

Received for publication, May 4, 2001, and in revised form, July 24, 2001
Published, JBC Papers in Press, July 26, 2001, DOI 10.1074/jbc.M104024200

Michael P. Rout^{‡§} and Mark C. Field^{¶||}

From the [‡]Laboratory of Cellular and Structural Biology, Rockefeller University, New York, New York 10021 and the [¶]Department of Biological Sciences, Wellcome Trust Laboratories for Molecular Parasitology, Imperial College of Science Technology & Medicine, London SW7 2AY, United Kingdom

Protozoan parasites of the order Kinetoplastida are responsible for a significant proportion of global morbidity and economic hardship. These organisms also represent extremely distal points within the Eukarya, and one such organism, *Trypanosoma brucei*, has emerged as a major system for the study of evolutionary cell biology. Significant technical challenges have hampered the full exploitation of this organism, but advances in genomics and proteomics provide a novel approach to acquiring rapid functional data. However, the vast evolutionary distance between trypanosomes and the higher eukaryotes presents significant problems with functional assignment based on sequence similarity, and frequently homologues cannot be identified with sufficient confidence to be informative. Direct identification of proteins in isolated organelles has the potential of providing robust functional insight and is a powerful approach for initial assignment. We have selected the nucleus of *T. brucei* as a first target for protozoan organellar proteomics. Our purification methodology was able to reliably provide both nuclear and subnuclear fractions. Analysis by gel electrophoresis, electron microscopy, and immunoblotting against trypanosome subcellular markers indicated that the preparations are of high yield and purity, maintain native morphology, and are well resolved from other organelles. Minor developmental differences were observed in the nuclear proteome for the bloodstream and procyclic stages, whereas significant morphological alterations were visible. We demonstrate by direct sequencing that the NUP-1 nuclear envelope antigen is a coiled coil protein, containing ~20 near-perfect copies of a 144-amino acid sequence. Immunoelectron microscopy localized NUP-1 to the inner face of the nuclear envelope, suggesting that it is a major filamentous component of the trypanosome nuclear lamina.

The most frequently studied eukaryote model systems are restricted to the metazoans, nematodes, and yeasts, which, from an evolutionary perspective, are a closely related subset of the kingdom (1–3). Although comparison between these systems is a powerful strategy for the elucidation of universal and unique cellular mechanisms, this approach is ultimately compromised by the relatively low divergence between these organisms. As the genomes of many economically and scientifically important divergent eukaryotes are becoming available, new challenges in functional genomics are emerging, requiring exploitation of novel strategies based on genome sequence and proteomic analysis.

Organisms of the order Kinetoplastida, which include the parasitic trypanosomatids *Leishmania* and *Trypanosoma*, separated from the metazoan lineage ~3 × 10⁹ years ago (3) and are the focus of much interest by virtue of their impact on both human morbidity and agriculture. *Trypanosoma brucei*, the causative agent of African trypanosomiasis, is responsible for ~100,000 deaths each year and is considered the third most important parasitic pathogen in overall economic impact (www.who.int/tdr/diseases/tryp). Trypanosomatids also represent one of the most divergent yet accessible experimental systems available. Several important features of eukaryotes were originally described in *T. brucei*, mainly on account of an extreme emphasis on these processes, for example eukaryotic polycistronic transcription, glycosylphosphatidylinositol anchoring of proteins, and kinetoplastids. The presence of specific functions or structures in either the protozoa or the higher eukaryotes has clear potential for the identification of therapeutic targets (4).

Although *T. brucei*, and related organisms, are comparatively cumbersome for genetic analysis, recent advances in gene disruption by RNA interference, genome projects, and proteomics provide potential strategies for rapid mapping of gene sequence to function (5, 6). One strategy relies on the comparison of gene sequences between organisms in order to identify functional orthologues. However, a major complication is that data base searches using regular algorithms frequently fail to identify such orthologues, due to low sequence conservation. Here we have taken a second approach, namely the direct identification of components of organelles and complexes by proteomic analysis of highly enriched specific subcellular fractions, which potentially avoids these difficulties.

Unfortunately, most methodologies only apply to a particular organism or a narrow subset of the Eukarya. We therefore attempted to modify our available techniques such that they would function for a highly divergent eukaryote, as an initial step toward making these methodologies more generally applicable. We chose to focus initially on the trypanosome nucleus

* This work was supported by international travel fellowships and program grant support from the Wellcome Trust (to M. C. F.); by the Rita Allen, Sinsheimer, and Hirsch Foundations; and by National Institutes of Health RO1 Grant GM62427-01 (to M. P. R.). The costs of publication of this article were defrayed in part by the payment of page charges. This article must therefore be hereby marked "advertisement" in accordance with 18 U.S.C. Section 1734 solely to indicate this fact.

§ To whom correspondence regarding fractionation may be addressed: Laboratory of Cellular and Structural Biology, Rockefeller University, 1230 York Ave., New York, NY 10021. Tel.: 212-327-8135; E-mail: rout@rockvax.rockefeller.edu.

|| To whom correspondence regarding trypanosomatids may be addressed: Dept. of Biological Sciences, Wellcome Trust Laboratories for Molecular Parasitology, Imperial College of Science Technology & Medicine, Exhibition Rd., London SW7 2AY, United Kingdom. Tel.: 44-202-7594-5277; E-mail: mfield@ic.ac.uk.

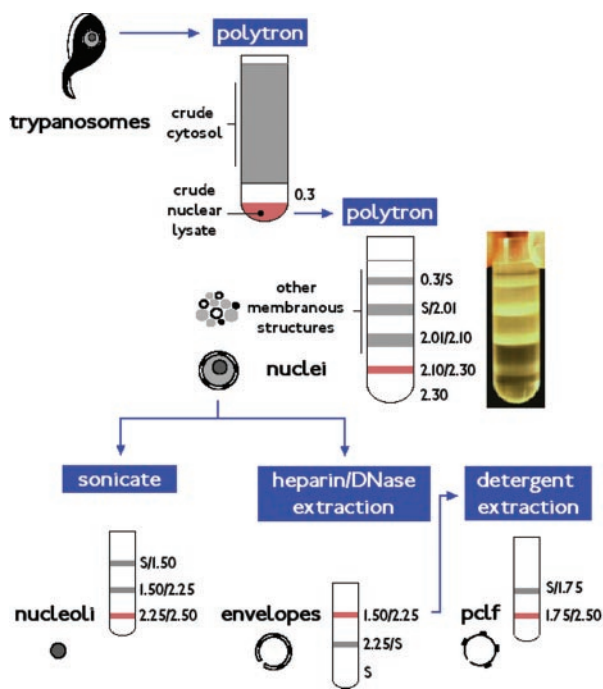


FIG. 1. Flow diagram demonstrating the relationship and origin of the various fractions produced in this study. Icons designating the major fractions (trypanosome, nuclei, nucleoli, NEs and PCF) are defined on this diagram and used throughout the display items as appropriate. Sucrose concentrations of the various gradient fractions, and the positions of the final products are indicated (see also "Experimental Procedures"). An example of a gradient for isolation of PCF nuclei manually supported by Dr. Field is also shown as *inset*. Gradient interfaces are indicated in gray, except those containing enriched nuclear or subnuclear fractions that are indicated in red.

and substructures, as this compartment has a number of available antibody markers and several identified protein components, in addition to representing an important system with a number of vital biological issues that may be resolvable by proteomic analysis. Unlike yeasts and metazoans, trypanosomatids transcribe their chromosomes in a polycistronic manner (7). This unusual feature suggests that these organisms use higher order chromatin structure and posttranscriptional control for regulation of gene expression (8, 9); hence, an understanding of trypanosome nuclear structure could provide profound insights into posttranslational control mechanisms in eukaryotes. In addition, the chromosomes never condense, and mitosis is closed, with an intact nuclear envelope present at all stages of the cell cycle (10). These organisms also appear to use unusual mechanisms for chromosome segregation (11). Further, several *T. brucei* protein coding genes, including the variant surface glycoprotein (VSG)¹ responsible for antigenic variation, are transcribed by RNA polymerase I, which is restricted to transcription of non-protein encoding genes in higher eukaryotes (12). Recent data suggest that a novel nucleolar-like compartment may be involved in polymerase I-mediated VSG transcription (13). Finally, a comparison of the composition and architecture of the trypanosome nuclear pore complex (NPC) and NE with those of other eukaryotes should shed light on the core conserved mechanisms of nucleocytoplasmic transport, NE assembly, and the organization of peripheral

(silent) heterochromatin (14).

We demonstrate the successful and reproducible isolation of nuclear, nucleolar, NE, and pore complex lamina fractions (PCLF) from *T. brucei*. The preparations are of high purity and yield, producing sufficient protein for the identification and characterization of specific organellar proteins. These methods provide a basis for the exploitation of proteomics approaches in this organism.

EXPERIMENTAL PROCEDURES

Materials—Buffer components and other reagents were from Sigma unless otherwise stated and of reagent grade or better. Culture media for trypanosomes and mammalian cells were from Life Technologies, Inc. and were sterilized by filtration. Fetal calf serum was heat-inactivated at 55 °C for 1 h before use.

Trypanosomes—Procyclic culture form or bloodstream form (BSF) trypomastigote (strain 427) trypanosomes were used throughout. Procyclic cells were cultured in 3.0-liter batches of SDM79 medium (15), supplemented with 10% fetal calf serum, 10 µg/ml hemin, 10 units/ml penicillin, 10 µg/ml streptomycin, in sterile 6-liter glass conical flasks, with gentle shaking (100 rpm) at 27 °C. Cells were allowed to attain a maximum density of 2–5 × 10⁷/ml before subculturing or harvesting. Bloodstream form trypanosomes were grown by infecting mice and rats and purified on DE-52 cellulose as described (16).

Antibodies—Mouse hybridoma cell lines secreting monoclonal antibodies against yeast nuclear envelope antigens were developed as previously described (17) and maintained according to Harlow and Lane (18). Antibody to the p67 protein and trypanosome BiP were the gift of Dr. James Bangs (University of Wisconsin, Madison, WI). Antibodies against trypanosome NE (NUP-1) and nucleolar (NUMAG) proteins were the kind gift of Prof. Keith Gull and Dr. Klaus Ersfeld (University of Manchester, Manchester, United Kingdom) (10). Antibody recognizing the trypanosome RNA-binding protein, RRM1, was from Prof. John Boothroyd (Stanford University, Palo Alto, CA) (19). Polyclonal rabbit antibodies against TbRAB2 have been described previously (20, 21). HRP-conjugated goat anti-rabbit immunoglobulin was from Sigma or Jackson Laboratories, HRP-conjugated donkey anti-mouse immunoglobulin was from Jackson Laboratories. A rabbit anti-mouse IgG bridging antibody was from ICN.

Isolation of Trypanosome Nuclei—Approximately 2.5 × 10¹⁰ to 7.5 × 10¹¹ procyclic cells were used for each nuclear isolation procedure. Cellular morphology and viability were verified beforehand by microscopy under an inverted tissue culture microscope (magnification, ×400). Cells were pelleted at 1700 × g_{av} for 10 min at 4 °C in a low speed centrifuge, resuspended in PBS (from Sigma PBS tablets) pre-chilled on ice, and repelleted. The cell pellet was transferred to an HB-4 tube (Sorvall) and pelleted once more in a swing out rotor benchtop centrifuge at 1800 g_{max} 4 °C for 15 min. All supernatant was carefully removed and the pellet placed on ice. 20 ml of 8% PVP (containing 0.05% Triton X-100 (Pierce SurfactAMPs grade), 5 mM Cleland's reagent, 100 µl of mammalian protease inhibitor mixture (Sigma), and 200 µl of solution P (100 mg of phenylmethylsulfonyl fluoride, 2 mg of pepstatin A in 5 ml of ethanol) was added per 2 × 10¹⁰ cells. The cell pellet was immediately processed with a precooled Polytron PTA-10 head, setting ~6, in 1–2-min bursts in the cold room. The lysate was cooled on ice between each Polytron bout. Lysis was followed by phase contrast microscopy (magnification, ×400) with an acceptable ~90% cell lysis usually occurring after a 5-min total Polytron treatment, although proportionately longer periods were required for larger volume lysates. The lysate derived from 2 × 10¹⁰ cells was underlaid with 10 ml of 0.3 M sucrose in 8% PVP plus 100 µl of solution P, 50 µl of 1 M DTT, and 50 µl of mammalian protease inhibitor mixture and then centrifuged at 11,000 × g_{av}, in an HB-4 rotor (Sorvall) at 4 °C for 20 min. The top layer (containing mainly cytosol, designated SN) was carefully decanted and stored at –80 °C. The crude nuclear pellet was immediately resuspended with 1-min bursts of the Polytron using setting 4.5 in a total volume (per 2 × 10¹⁰ cell eq) of 8 ml of 2.1 M sucrose in 8% PVP, 50 µl of 1 M DTT, 50 µl of mammalian protease inhibitor mixture, and 100 µl of solution P. Close to 100% cell dispersal is achieved at this point, with no detectable nuclear damage. ~12 ml of this suspension was loaded per SW28 tube (Beckman) containing a discontinuous step gradient (from the bottom, 8 ml of 2.30 M sucrose/PVP, 8 ml of 2.10 M sucrose/PVP, 8 ml of 2.01 M sucrose/PVP, all containing protease inhibitors) (17, 22, 23). For the preparation to be successful, it is essential that no more than 2.5 × 10¹⁰ cell eq be loaded into each SW28 tube. The gradient was centrifuged at 100,000 × g_{av}, in

¹ The abbreviations used are: VSG, variant surface glycoprotein; BSF, bloodstream form; NE, nuclear envelope; NPC, nuclear pore complex; PBS, phosphate-buffered saline; PCF, procyclic culture form; PVP, polyvinylpyrrolidone; PCLF, nuclear pore complex lamina fraction; HRP, horseradish peroxidase; EM, electron microscopy; DTT, dithiothreitol; OD, optical density; PAGE, polyacrylamide gel electrophoresis; ER, endoplasmic reticulum; GSS, genome survey sequence.

TABLE I
Protein fractionation during nuclear and subnuclear isolation procedures

The leftmost column (Organelle) indicates the fraction most enriched in the named organelle or substructure generated during the procedures (see "Experimental Procedures" and Fig. 1), while the second column (Fraction) indicates the fractions obtained during the isolation procedure by their position on the relevant sucrose gradient (see Fig. 1). The third column (Total protein) indicates the amount of total protein in each fraction, expressed as a percentage (%) relative to the total amount of protein in the starting whole cell pellet. The protein in each fraction was quantitated by the Bradford method or by densitometry of Coomassie Blue-stained SDS gels, and the two results averaged to generate the figure given (see "Experimental Procedures"). The rightmost six columns indicate the incidence of the indicated marker protein in each fraction, expressed as a percentage (%) relative to the amount of that marker present in whole cells as quantitated by densitometry of ECL signals on films (see "Experimental Procedures"). ER, endoplasmic reticulum; Lys, lysosome; Nuc, nucleus; Nucl, nucleolus; NE, nuclear envelope.

Organelle	Fraction	Total protein	Marker					
			TbBiP (ER)	p67 (Lys)	TbRAB2 (ER)	RRM1 (Nuc)	NUMAG (Nucl)	NUP-1 (NE)
		%	% of total					
Nuclei	S/N	46	26	27	56	12	0	0
	0.3/S	19	25	23	19	12	0	4
	S/2.01	19	23	27	19	13	7	8
	2.01/2.10	9	12	17	2	20	9	11
	2.10/2.30	8	14	6	4	43	84	77
Nucleoli	S/1.50	3				24	23	44
	1.50/2.25	3				12	27	20
	2.25/2.50	2				7	34	13
NE	S	3				22	28	7
	2.25/S	3				13	30	17
	1.50/2.25	2				8	26	53
PCLF	S + S/1.75	1				5	17	13
	1.75/2.50	1				3	9	40

a SW28 rotor for 3 h at 4 °C and immediately unloaded from the top, and fractions were examined by phase contrast microscopy (magnification, $\times 1000$). The nuclei were recovered at the 2.10/2.30 interface and stored at -80 °C. Nuclei, and other subfractions, are stable morphologically at -80 °C for at least 18 months. Nuclei can be conveniently quantitated at this stage by optical density (OD) at 260 nm; for *T. brucei*, 1 OD_{260 nm} corresponds to $\sim 10^8$ nuclei, and has an OD_{260 nm}/OD_{280 nm} ratio of ~ 1.3 .

For bloodstream form cells, nuclei were isolated in a similar manner, with the exceptions that cells were harvested in trypanosome dilution buffer (16), and that Tween 20 (SurfactAMPs grade, Pierce) was added to 0.05% to the lysate for Polytron resuspension of the crude nuclear pellet.

Preparation of Nucleoli— ~ 50 OD_{260 nm} of purified nuclei were diluted by the addition of 0.2 volumes of 8% PVP and pelleted at $170,000 \times g_{av}$ for 1 h at 4 °C in a type 80 rotor. The supernatant was discarded and 1 ml of 10 mM Bis-Tris-Cl, pH 6.50, 0.6 mM MgCl₂, 0.5 mM DTT, 0.34 M sucrose, 0.05% Tween 20 (SurfactAMPs), 5 μ l of solution P, and 5 μ l of mammalian protease inhibitor mixture (Sigma) was added. The nuclei were then disrupted by sonication with a microprobe in 6-s bursts with cooling of the probe and lysate on ice between bursts. Disruption of the nuclear structure and generation of nucleoli was monitored between each successive sonicator burst by phase contrast microscopy (magnification, $\times 1000$). A total of six sonicator bursts was normally found to be sufficient to achieve $>99\%$ nuclear disruption. The sonicate was then mixed 1:1 with 1.75 M sucrose in 10 mM Bis-Tris-Cl, pH 6.50, 0.1 mM MgCl₂, (BT/Mg) and layered onto a step gradient in an SW55 tube (Beckman) consisting of 1 ml of 2.50 M sucrose, 1.5 ml of 2.25 M sucrose, and finally 1.5 ml of 1.75 M sucrose all in BT/Mg (24). The gradient was then centrifuged at $240,000 \times g_{av}$ for 2 h at 4 °C in an SW55Ti rotor. Nucleoli were recovered at the 2.00 M/2.50 M interface.

Nuclear Envelope Fraction—300 OD_{260 nm} of purified *T. brucei* nuclei were diluted with 0.2 volumes of 8% PVP solution and pelleted in a Ty50.2Ti rotor (Beckman) at $140,000 \times g_{av}$ at 4 °C for 1 h. The nuclear pellet was resuspended in 3 ml (per 100 OD of nuclei) of nuclear lysis solution (BT/Mg, 1 mM DTT, 1.0 mg/ml heparin, 20 μ g/ml DNase I (DN-EP, Sigma), 2 μ g/ml RNase A (Roche Molecular Biochemicals), 1:100 solution P, 1:200 mammalian protease inhibitors) by vortexing vigorously at room temperature until at least 1 min after the last traces of the pellet had dispersed. The suspension was incubated for an additional 5 min at room temperature before being diluted with 12 ml of 2.10 M sucrose, 20% Accudenz (Accurate Chemical Scientific Corp.), BT/Mg, and mixed thoroughly. This mixture was placed in a SW28 tube (Beckman) and overlaid with 12 ml of 2.25 M sucrose, BT/Mg, and then 10 ml of 1.50 M sucrose, BT/Mg and centrifuged at $100,000 \times g_{av}$, for 4 h at 4 °C. The NEs are recovered primarily from the 1.50 M/2.25 M interface and can be visualized as faint "C"-shaped structures by phase contrast microscopy.

Nuclear Pore Complex Lamina Fraction—One volume of the NE

fraction was diluted with 2 volumes of 1.5% Triton X-100, 1.5% sodium taurodeoxycholate, 10 mM Bis-Tris-Cl, pH 6.50, 1:100 solution P, and 1:500 mammalian protease inhibitors. This mixture was vortexed for 5 min at room temperature and incubated for another 25 min at room temperature. Three milliliters of the mixture was then overlaid in a SW55 tube (Beckman) containing a step gradient of 1.0 ml of 2.50 M sucrose, BT/Mg and 1.0 ml of 1.75 M sucrose, BT/Mg, which was then centrifuged for 30 min at $240,000 \times g_{av}$, and 4 °C. The resulting nuclear pore complex lamina fraction was recovered at the 1.75 M/2.50 M interface.

Electron Microscopy—Samples were prepared for negative stain with uranyl acetate as described (17). For thin section EM, nuclei were prepared by dilution into an equal volume of 0.6 M sucrose, 8% PVP, followed by 10% EM grade glutaraldehyde to a final concentration of 2.0%. Nucleoli and envelope preparations were diluted into an equal volume of 1 M sucrose, 10 mM Bis-Tris-Cl, pH 6.5, 1.0 mM MgCl₂ and then fixed by addition of 10% glutaraldehyde to 2%. Fixation was overnight at 4 °C, followed by pelleting in a Ti45 rotor at 40 000 rpm for 1 h at 4 °C. Pellets were then washed in a minimum volume of sodium phosphate/MgCl₂ buffer at 4 °C, overnight prior to embedding and osmification. For immunoelectron microscopy, NEs were processed exactly as described (25, 26) using a 1:5 dilution of monoclonal antibody NUP-1 as the first antibody. EM images were acquired on a JEOL 510.

SDS-PAGE—SDS-PAGE analysis was performed on methanol precipitated proteins. Protein samples were first precipitated by addition of methanol ($>5 \times$ sample volume) and incubation at 4 °C for at least 1 h, followed by washing with 70% methanol (v/v). Proteins were solubilized by heating in reducing sample buffer at 75 °C, and resolved by electrophoresis through precast 4–20% gradient polyacrylamide gels (Novex) at 50 V for 10 min, followed by 120 V for 90 min. Broad range molecular mass markers were from Bio-Rad. Proteins were visualized by Coomassie Blue staining. In some instances, proteins were transferred to nitrocellulose by wet blot (18). Gels were documented by scanning at greater than 300 dpi, and manipulated in Adobe Photoshop version 5.0 for presentation. For analysis of gradient fractions, samples were normalized to cell equivalents by differential loading.

Extraction and Analysis of DNA from Nuclei and Nucleoli—Material for extraction was pelleted in a TL100 ultracentrifuge in a Ti50 rotor for 1 h at $100,000 \times g_{av}$, and resuspended in 0.4 ml of 10 mM Tris-HCl, pH 8.0, containing 2% Triton X-100, 1% SDS, 100 mM NaCl, 1 mM EDTA. DNA was then extracted and separated on agarose gels using standard methods. For removal of RNA, aliquots of the preparation were digested with RNase A at 50 μ g/ml at room temperature for at least 1 h.

Western Blot Analysis—Filters were blocked in 2% freeze-dried milk in Tris-buffered saline containing 0.1% Tween 20 (18). Monoclonal antibody culture supernatants were used at 1:5 to 1:100 in 2% milk/Tris-buffered saline containing 0.1% Tween 20, with a rabbit anti-mouse IgG bridging antibody followed by a goat anti-rabbit HRP conjugate at 1:10000, followed by Luminol reagent. All antibodies for

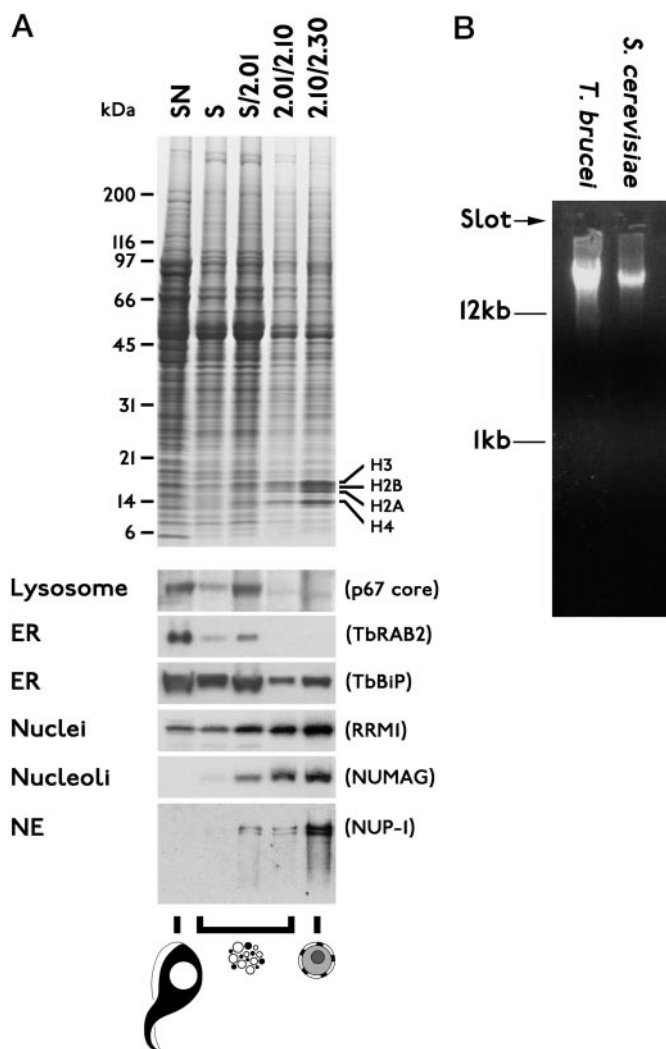


FIG. 2. Analysis of trypanosome nuclear isolation procedure by SDS-PAGE and Western blot. A, Coomassie Blue-stained SDS-PAGE separations of the fractions from a representative PCF nuclear isolation are shown in the *top panel*, and corresponding Western blots are shown *below*. Note that loading volumes have been adjusted for cell eq, facilitating quantitative comparison between the *lanes*. *Icons* correspond to those used in Fig. 1. Antibodies used are indicated at the *right* of the blot images, and the compartments that they predominantly recognize are given at *left*. The relative migration positions of the trypanosome histones are indicated (32). Molecular size standards are shown at left in kDa, and sucrose gradient fraction designations above the corresponding lanes. SN, supernatant from first centrifugation (mainly cytosol); S, supernatant from second gradient at the loading zone. S/2.01, 2.01/2.10, and 2.10/2.30 are the retrieved fractions spanning the interfaces between the various sucrose bands. The nuclear antigens NUP-1, NUMAG, and RRM1 are significantly enriched in the 2.10/2.30 fraction, which contains the vast majority of nuclei, while the ER proteins TbBiP and TbRAB2 and the lysosomal protein p67 are depleted from this fraction. B, DNA extracted from trypanosome and yeast nuclei and fractionated on a 0.9% agarose gel and stained with ethidium bromide. DNA is exclusively very high molecular weight, suggesting that the chromatin structure is well preserved during the isolation procedure.

analysis of nuclear fractionations were used in Western analysis at 1:100 to 1:1000 in 2% milk/PBS plus Tween 20 and were incubated for 1 h at room temperature. The blots were exposed on Kodak Biomax film and documented as above for gels.

Bioinformatics—Sequences corresponding to 26 *Saccharomyces cerevisiae* and 15 mammalian nucleoporins and NPC-associated proteins were used to search the *T. brucei* data bases at TIGR unfinished genomes (www.tigr.org/) and Sanger parasite blast server (www.ebi.ac.uk/parasites/parasite_blast_server.html) on 25–26 November 2000 via an 802.11b link. Searches were performed using the full-length or partial protein sequences and tBLASTp on the remote server, using

default parameters. All putative hits were inspected by eye following retrieval. Identification of GSS entries encoding NUP-1 were obtained by tBLASTn at the Sanger parasite blast server and assembled using ClustalX. Coiled-coil prediction was made using MacStripe 2.0a1 using the default settings (28).

Quantitation—Protein concentrations were determined by the Bradford method or by densitometry of Coomassie-stained SDS-PAGE samples. Semiquantitative data for selected trypanosome marker proteins were obtained by high resolution scanning at 24 bits of Coomassie-stained gels or ECL-exposed films following Western blotting.

Protein Sequence Determination—A protein doublet band of the nuclear pore complex lamina fraction with a M_r of ~350,000 was selected for microsequencing based on its abundance, separation from other proteins of the fraction and cofractionation during the enrichment procedure. Proteins of this fraction were separated by SDS-PAGE and transferred electrophoretically to polyvinylidene difluoride membrane. The ~350-kDa protein was visualized on the membrane with 0.1% Amido Black in 10% acetic acid, excised, cleaved with endopeptidase Lys-C (28), and the peptides subjected to NH_2 -terminal sequence analysis. High abundance proteins coenriching with the nucleus and migrating in the histone region of the gel were also analyzed.

RESULTS AND DISCUSSION

Identification of Trypanosome Nuclear Components by Comparative Methods—To identify components of the trypanosome nucleus, we screened a panel of ~100 monoclonal antibodies raised against highly purified yeast NE fractions (24). Only one hybridoma gave significant reactivity (data not shown). We also searched the trypanosome data bases against 41 yeast and vertebrate nucleoporin protein sequences (reviewed in Ref. 29). In contrast to confident identification of TbRAN (30), these searches were largely unsuccessful; regions of homology were restricted to repeat-containing domains, preventing unambiguous assignment of orthology. These data dramatically underscore the extreme divergence between trypanosomes and higher eukaryotes and indicate that direct analysis, by isolation and proteomics, is likely to be a requirement for a complete characterization of divergent eukaryote organelles.

Isolation of Enriched Nuclear Fractions from Trypanosomes—We used as a starting point the isolation procedure for *S. cerevisiae* nuclei developed previously (17, 22, 23). This method is reliable and capable of obtaining nuclei in high yield and of a quality sufficient for subsequent subfractionation and proteome analysis (see Refs. 14 and 31, and references therein), and in addition was potentially adaptable to trypanosomes. We chose this method over several other protocols on the grounds that rigorous morphological and purification data were generally unavailable for the latter.

Our modified procedure involves a Polytron lysis followed by the separation of soluble and membranous material by centrifugation. The nuclei are then isolated from the other membranous structures on a sucrose step gradient. The procedure is easily completed in 1 day and is shown in schematic form in Fig. 1. The final nuclear fraction, recovered at the 2.10/2.30 m sucrose interface, was in very high yield and purity, and is clearly visible in the image of a typical step gradient (*inset*). Release of chromatin or nuclear rupture was negligible during the isolation procedure. Additionally, we found that the procedure was scalable; excellent results were obtained with starting cell numbers ranging over 2 orders of magnitude, *i.e.* from 10^{10} to 10^{12} procyclic form parasites.

We also isolated nuclei from BSF *T. brucei* trypomastigotes, with a minor additional modification of the procedure (see “Experimental Procedures”). Increased flocculant behavior was observed for the bloodstream form membranes during the initial lysis (data not shown), most probably due to extensive stripping of the exoplasmic leaflet of VSG (below). Addition of small quantities of the nonionic detergent, Tween 20, were sufficient to facilitate isolation of BSF nuclei.

Analysis of Isolated Trypanosome Nuclei—Most analysis fo-

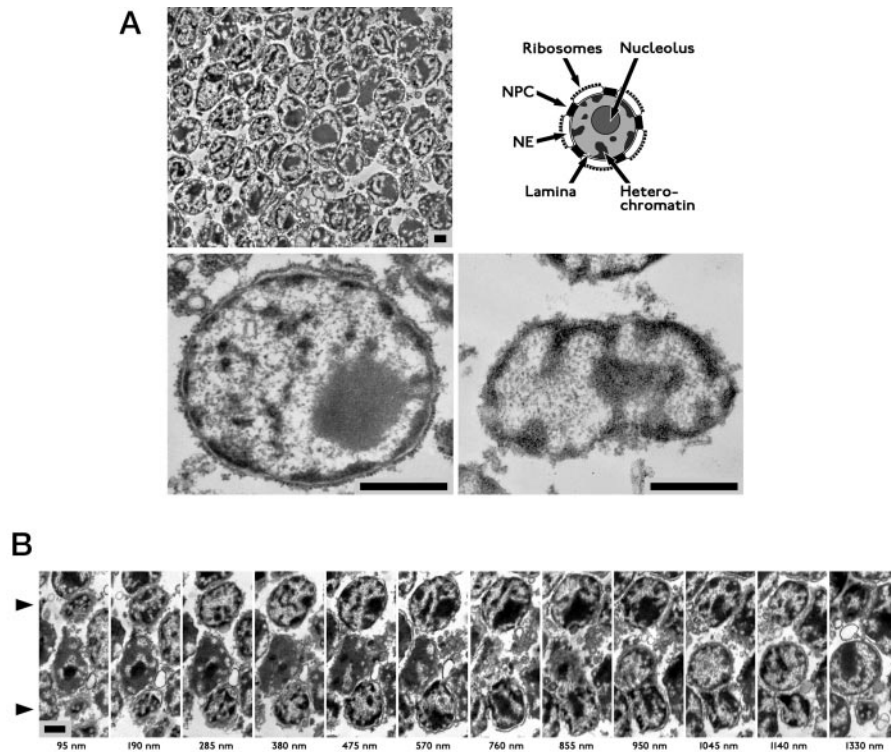


FIG. 3. Electron microscope analysis of the nuclear fraction obtained from *T. brucei*. *A*, *top left panel*, low magnification of a typical field from a thin section of the material from the 2.10/2.30 interface. The high abundance of intact nuclei and the near complete absence of contaminating structures is good evidence for a high purity isolation, and is consistent with the analysis shown in Fig. 2. *Top right panel* shows a schematic highlighting the various nuclear features that are easily visible in the nuclei, particularly in the PCF example (*lower left*). *Lower panels*, procyclic culture form (*left*) and bloodstream form (*right*) nuclei at higher magnification. Note the clear differences in the morphology of the nuclei from the two life stages. The PCF nucleus is rounded, with a resolved NE and a large nucleolus, whereas the nucleus from the BSF is irregular in shape, has a less distinct NE and a smaller nucleolus. In addition, in the PCF the arrangement of the heterochromatin is into small regions, some of which are associated with the NE; this latter heterochromatin is excluded from the regions subtending the NPCs. In the BSF nucleus, the heterochromatin is rather more contiguous, and predominantly associated with the NE. *Scale bar* = 0.5 μm . *B*, serial sectioning of PCF nuclei. These sections demonstrate that there is a single nucleolus, and that the heterochromatin forms a clear interconnected network, especially visible in the nuclei indicated in the first section of the series with arrowheads. The nucleolus occupies $\sim 15\%$ of the nuclear volume, and a similar proportion is taken by heterochromatin. Section depths into the sample are indicated *below each panel*; *scale bar* is 0.5 μm .

cused on PCF nuclei as this life stage is easier to culture in large numbers. Isolation of the nuclei results in removal of $\sim 90\%$ of the total cellular protein (Table I). SDS-PAGE analysis demonstrated a high degree of enrichment for certain protein bands in this fraction (Fig. 2), particularly a complex of low molecular weight composed mainly of trypanosome histones, based on mobility (32) and peptide sequence data (Fig. 9). In BSF preparations, VSG was recovered mainly in the first supernatant as a prominent band at ~ 65 kDa, indicating conversion to the sVSG form by hydrolysis of the glycosylphosphatidylinositol anchor following release of cytoplasmic glycosylphosphatidylinositol phospholipase C during lysis (33). VSG was almost completely absent from the nuclear fraction (data not shown). Extraction of DNA from isolated procyclic nuclei and analysis by agarose gel electrophoresis revealed that the DNA was of very high molecular weight (Fig. 2B), suggesting that the chromatin was essentially undamaged.

We analyzed the gradient fractions for the presence of a number of proteins predicted to purify with the nucleus, as well as a group of proteins localized to other compartments (Fig. 1). The nuclear proteins examined were RRM1, an RNA-binding protein (19); NUP-1, an NE marker; and NUMAG, a nucleolar protein (10). In all three cases these proteins were strongly enriched in the nuclear fraction (Table I), indicating a total nuclear recovery of nearly 80%. By contrast, no significant TbRAB2 was detected in the nuclear fraction, consistent with this protein being associated with the cytosolic face of the ER, and binding to the membrane in a reversible manner (20).

TbBiP was mainly recovered in lighter fractions, consistent with an ER luminal location (34), but a significant fraction was associated with the nucleus, due to the presence of this protein in the perinuclear cisternae (20).

We next examined the fractions by thin section EM (Fig. 3). Clear flagellar and vacuolar structures, including putative flagellar pocket structures, could be seen in the topmost fractions (data not shown), but are rare in the nuclear fraction. In addition the nuclei are morphologically intact, each with a preserved double membrane, extensive nucleolar and heterochromatin regions, and NPCs within the NE (10). There is also a structure that resembles a nuclear lamina associated with the inner face of the nuclear membrane (35), consistent with the robust behavior of the nuclei during the isolation procedure as the trypanosome nuclei are significantly less fragile than yeast nuclei (which lack a lamina). Together, these data demonstrate the integrity and high degree of enrichment of the isolated trypanosome nuclei.

Strikingly, the overall shapes of the released nuclei were different for the two stages. Isolated procyclic nuclei are close to spherical, but nuclei from bloodstream form cells are significantly more elongated (Fig. 3). Similar developmental features have been observed previously by other workers in intact trypanosomes. The present observations indicate that the shape of the nucleus is due to organization of the nuclear matrix, and not the cytoskeleton or repositioning of the organelle during development.

Extensive electron-dense regions corresponding to hetero-

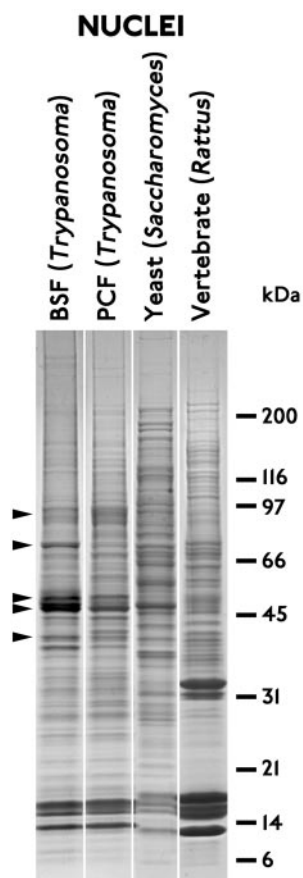


FIG. 4. Developmental and species-specific protein expression in the nucleus. Proteins from highly purified nuclei are shown resolved by SDS-PAGE on 4–15% gradient gels, and visualized by Coomassie staining. A few significant differences are apparent between the two *T. brucei* life stages (*left pair of lanes*), the most prominent of which are indicated by *arrowheads* at the *left* of the *panel*. The overall high degree of constitutive expression in the trypanosome suggests that the rather striking morphological alterations observed in Fig. 3, and the life-stage dependent alterations to chromatin structure and gene expression, are mediated by a restricted subset of proteins. Rather more extensive alterations in the protein compositions between the trypanosomatids and the other eukaryote nuclei are visible (*right pair of lanes*), but the abundant low molecular weight complex corresponding in part to histone proteins is present in all preparations. Migration positions of molecular size markers are indicated at the *right* in kDa.

chromatin and the nucleolus are visible in the nuclei, consistent with previous studies (10, 36). The most prominent feature of both BSF and PCF nuclei is the large nucleolus. This structure is extremely electron dense with no discernible internal organization. In the PCF the nucleolus is compact whereas in the BSF it is more irregular. There is clear heterochromatin-like material associated with the periphery, but each heterochromatin region is rather more extensive in the BSF nuclei. Compared with their bloodstream counterparts, PCF nuclei contain larger numbers of smaller heterochromatin regions (Fig. 3, A and B), consistent with a reorganisation of chromatin during differentiation from the BSF to the PCF (8, 11, 32, 37, 38). In addition, small amounts of material with similar electron density to heterochromatin were observed in close juxtaposition to the nucleolus. In the procyclic nuclei the differentiation between the inner and outer NE is well defined, making the presence of NPCs clear in transverse section (39). For the majority of NPCs, heterochromatin is excluded from the region immediately adjacent to the NPC, as has been observed in many other organisms (39). Serial sectioning, together with negative stain EM images, allowed a morphometric analysis of the PCF nuclei. These nuclei have overall dimensions of $1.9 \times$

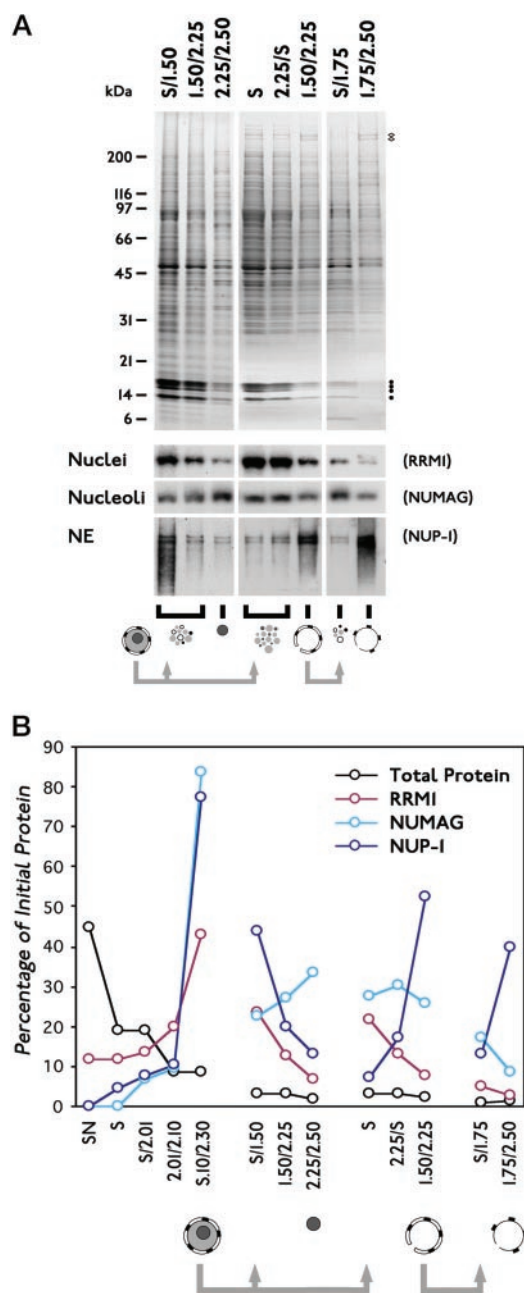


FIG. 5. Analysis of trypanosome subnuclear fractionation procedures by SDS-PAGE and Western blot. A, Coomassie Blue-stained one-dimensional SDS-PAGE separations of the fractions from representative PCF subnuclear fractionations are shown in the *top panel*, and corresponding Western blots are shown *below*. *Icons* correspond to those used in Fig. 1; *gray arrows* indicate the derivation of the nucleolar, NE, and PCLF fractions from preceding fractions. Antibodies used are indicated at the *right* of the blot images (RRM1, NUMAG, and NUP-1), and the compartments they predominantly recognize are given at *left*. Molecular size standards are shown at *left* in kDa, and sucrose gradient fraction designations given *above* the corresponding *lanes*. The *leftmost three lanes* are the nucleolar isolation, the *center three* the NE preparation, and the *rightmost two lanes* are the PCLF purification. Coenrichment of the nucleolar marker NUMAG is clear for the nucleoli preparation, and enrichment for the NE marker NUP-1 is similarly significant for the isolation of the NE and PCLF. Note the comparative simplicity of the protein compositions of the final fractions, and the removal of the majority of the histone complex (positions indicated to the *right* of the gel with *filled circles*). The 350-kDa doublet recognized by the NUP-1 antibody is clearly visible in the 1.50/2.25 and 1.75/2.50 fractions (positions indicated to the *right* of the gel with *open diamonds*). B, quantitation of total protein and RRM1, NUMAG, and NUP-1 yields from the nuclear and subnuclear isolation procedures. Sucrose gradient fraction designations and icons are as in Fig. 1. Data are represented as a percentage of the protein present in the relevant starting material.

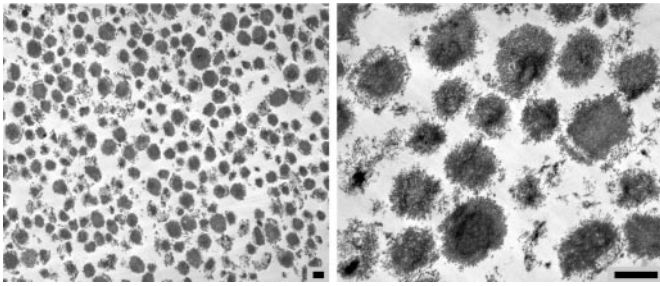


FIG. 6. Ultrastructural analysis of the nucleolar fraction prepared from *T. brucei* nuclei. Representative EM images of the final nucleolar preparation are shown at low (*left panel*) and high (*right panel*) magnification. The nucleoli are heterogeneous in size, which may reflect a real variability in the structure of this organelle based on cell cycle position and other parameters, but this probably also arises in part from fragmentation of the structure during isolation. Note that nucleoli contain a highly compacted central core region, with a less dense peripheral region; this is also seen in images of nucleoli within the intact PCF nuclei. Some of the nucleoli are associated with peripheral material, which is most likely chromatin and nuclear matrix remnants. Scale bars = 0.5 μm .

1.5 μm , and from tangential sections there are 200–300 nuclear pores/nucleus.

We also compared the nuclear proteome of PCF and BSFs with each other, *S. cerevisiae* and vertebrates (*Rattus norvegicus*) by one-dimensional SDS-PAGE (Fig. 4). The analysis demonstrated that the protein composition of the trypanosome nuclei does not vary greatly between life stages, with the vast majority of bands being in common. However, a minor fraction of the bands were altered in intensity and are good candidates for developmentally regulated nuclear proteins. The overall similarity in the protein profiles of BSF and PCF nuclei reflects the majority of nuclear protein being structural and involved in chromatin/matrix assembly and maintenance with only a very minor fraction responsible for control of differential gene expression and other stage specific functions. By contrast a very significant difference in the protein electrophoretograms for the three species is seen; this may in part be due to alterations in the migration of homologous nuclear proteins, but probably also reflects real differences in protein composition. Significantly, a similar high abundance low molecular weight complex, consisting mainly of histone proteins, was present in all three species.

Having obtained high quality nuclei, we sought to isolate subnuclear fractions for further analysis. We focused on nucleoli, NEs, and the PCLF. The unusual role of polymerase I made production of nucleoli an important goal, while the latter fractions are vital for production of NPCs and associated structures suitable for both proteomic and morphological analysis (26, 40). As a starting point, we used the purified nuclei from the pro-cyclic stage.

Isolation of Nucleoli from Trypanosome Nuclei—Using microprobe sonication, nucleoli were liberated from the nuclei and recovered on a sucrose step gradient by modifications of a procedure originally developed for isolation of nucleoli from rat tissues (41) (Fig. 1). SDS-PAGE analysis of the nucleoli preparation revealed that the nucleolar fraction recovered at the 2.25/2.50 sucrose interface was significantly depleted of a number of proteins, and in particular the low molecular weight histone complex (Fig. 5A). The nucleolus fraction contained ~25% of the total nuclear protein. Western analysis, using the three nuclear antigens described earlier, revealed that RRM1 and NUP-1 were significantly depleted from the nucleoli, whereas by contrast NUMAG, the nucleolar antigen, was moderately enriched, with ~40% of the nuclear signal recovered in the 2.25/2.50 fraction (Table I; Fig. 5B). Light and electron

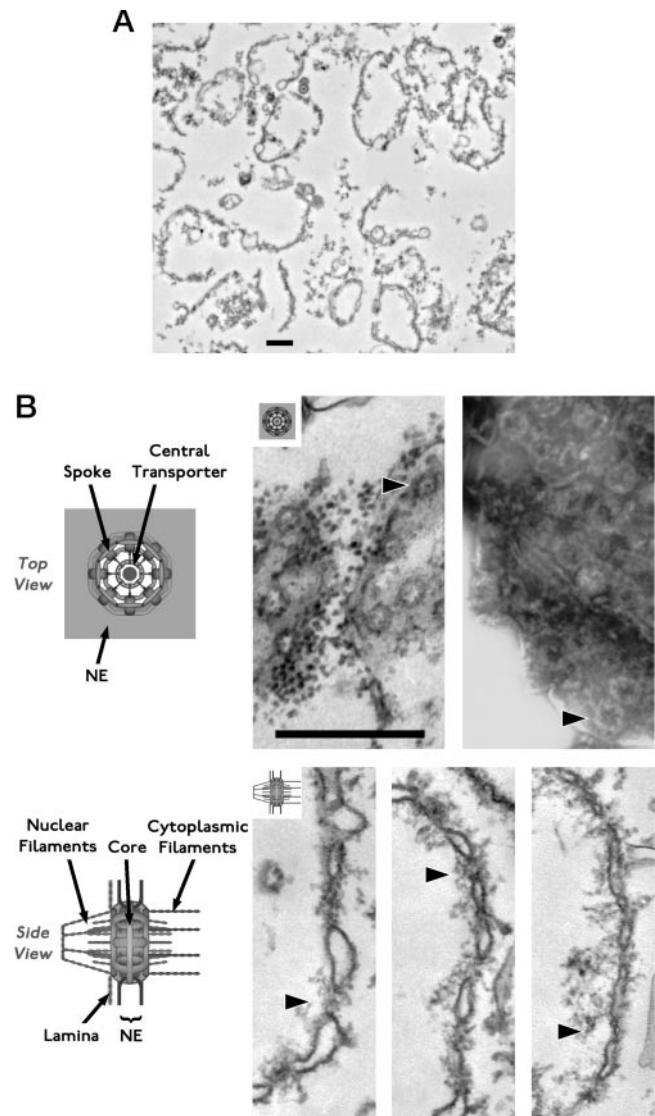


FIG. 7. Ultrastructural analysis of the nuclear envelope fraction prepared from *T. brucei* nuclei. A, low magnification electron micrograph of isolated NEs. Note the near absence of nucleoplasmic material (chromatin and nucleolus) from these preparations. Clearly visible are the inner and outer nuclear membranes, and also electron-dense structures arrayed along the nuclear envelopes, which correspond to NPCs. B, high magnification electron micrographs demonstrating detailed ultrastructure of the trypanosome NE. Schematics showing visible features of the NPC are shown at the left of the figure. *Top panels* are *en face* views of the NEs. The *left-hand* micrograph is a tangential section, clearly revealing the ring structure of the NPCs, and in some instances a central plug and spoke elements can be seen (*arrowhead*). Ribosomes studding the outer face of the NE are apparent in the *center* of the micrograph. The *right-hand* image is a negative stain preparation; again, features of the NPC can be discerned. Note the high density of the NPCs, especially clear in the negative stain image. *Lower panels* are cross-sections of NEs and again reveal details of the NPC architecture. Clearly visible are the cytoplasmic and nuclear filaments, the central core elements, and electron-dense material corresponding to the main ring structures. Good examples are indicated in the *leftmost two panels* by *arrowheads*. In the *right panel* a clear filamentous network is seen associated with the inner nuclear membrane and which may constitute the trypanosome nuclear lamina (*arrowhead*). *Insets* show the same schematics as the *left* but reduced to scale. Scale bar = 0.5 μm .

microscopy assays indicated a much higher recovery of nucleoli in the final fraction: greater than 80% of those present in the starting nuclear material. NUMAG may be preferentially lost in our procedure; alternatively, like many nucleolar components, it may be dynamically localized to the nucleolus, result-

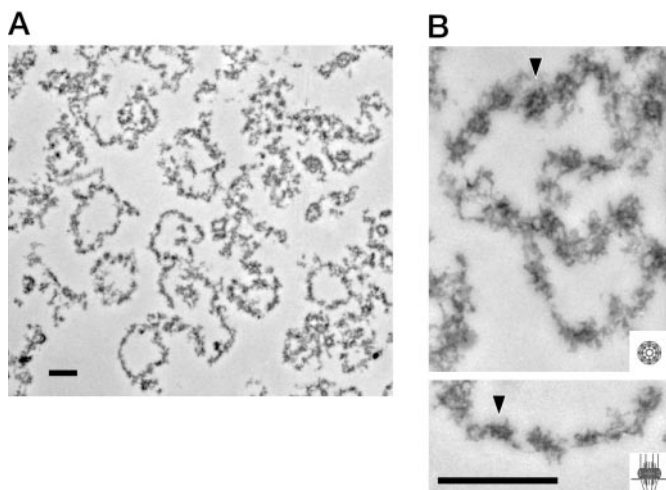


FIG. 8. Ultrastructure of the nuclear pore complex lamina fractions prepared from *T. brucei* nuclei. *A*, low magnification EM image of the PCLF. The majority of the membranous material has been removed, and the NPCs are visible again as electron-dense punctata (compare this image with the one in Fig. 7A), but the overall integrity remains, indicating a robust lamina structure is present. *B*, high magnification electron micrographs showing details of the NPC structures; again, a central core and peripheral filamentous structures are clearly visible. Note that the ribosomes, visible in earlier fractions as small dense dots, have been completely removed, consistent with an efficient extraction of membrane elements. *Insets* contain schematics of the NPC to scale, *en face* (top) or in cross-section (lower). Scale bar = 0.5 μ m.

ing in the presence of a significant fraction in the nucleoplasm. Furthermore, some of the NUMAG recovered in lighter fractions may be associated with the extranucleolar compartment recently detected in *T. brucei* nuclei (13), which is unlikely to sediment as rapidly as the larger nucleoli. The majority of nuclear matrix was depleted, as evidenced by the loss of RRM1. EM demonstrated that the nucleoli were comparatively homogeneous (Fig. 6), consisting of spherical structures of densely packed material, similar to the appearance of nucleoli in both intact trypanosomes and in the isolated nuclei (Fig. 3).

Isolation of the Nuclear Envelope and a Pore Complex Lamina Fraction from Trypanosomes—Nuclear envelopes and the nuclear pore complex lamina fraction were isolated in a sequential procedure, with the envelope fraction acting as the starting point for the pore complex lamina preparation. The trypanosome NE preparation methodology is based on that for yeast NEs (24, 42). Again, SDS-PAGE analysis indicated a significant alteration in the protein compositions of the final fractions (Fig. 5). There was a significant loss of histone complex from the envelope preparation. In addition a high molecular mass doublet, at \sim 350 kDa, was enriched in this fraction. Western blot analysis indicated a depletion of RRM1 and NUMAG and a clear enrichment of the NUP-1 antigen. From these analyses it became clear that the NUP-1 antigen comigrated with the 350-kDa doublet, suggesting that they may be the same molecule (Fig. 5). Based on these data, we estimate that the NE fraction recovered $>70\%$ of the NEs released from the nuclei, whereas depletion of NUMAG, RRM1, and the histone bands from this fraction contests to a low level of nucleoplasmic and nucleolar contamination (Table I; Fig. 5).

Isolated NEs frequently adopted a characteristic C profile in EM sections (24), and were devoid of significant amounts of chromatin (Fig. 7A). The appearance of these fractions was rather more heterogeneous than for the isolated nuclei and nucleoli. The envelopes were clearly quite extensive when visualized by negative stain. Both the inner and outer nuclear membranes were resolved, and in some regions less closely juxtaposed than the equivalent structures in the intact nuclei,

possibly because of relaxation of the envelope due to removal of the nuclear contents. The outer membrane was studded with large numbers of particles of the correct size and morphology for ribosomes. The envelopes exhibit a very high density of NPCs, prominently seen as regions where the inner and outer membrane are in close juxtaposition. Fibrous material was visible on both the cytoplasmic and the nuclear side of the NPC; at this level of resolution, the trypanosome NPC displays an organization that is indistinguishable from higher eukaryote NPCs (43). The NPCs themselves averaged \sim 110 nm (diameter) \times 50 nm thick (for the densely staining core), with filaments extending \sim 50 nm into nucleoplasm and cytoplasm. By negative stain (Fig. 7B), the high density of the NPCs is even clearer and, for a number of the complexes, an 8-fold symmetry can be discerned, consisting of spokes surrounding a central element (39). Hence, the basic NPC architecture is indeed conserved between crown eukaryotes and divergent organisms like trypanosomes.

The pore complex lamina fraction was derived from the NEs by a detergent extraction. The protein composition of this fraction was somewhat simplified from the NEs and contained \sim 50% of the NE protein. This final material contained most (\sim 75%) of the NUP-1, consistent with the stable association of NUP-1 with the NPC or lamina. In addition, both RRM1 and NUMAG were depleted from the pore complex lamina, indicating further removal of trace contaminating nucleoplasmic material. By EM the NPCs are clearly visible in the PCLF, with an 8-fold symmetry, a central plug, and peripheral filaments, indicating that the morphology is well preserved (Fig. 8, A and B). Significantly, the NPCs are interconnected by a clear, fibrous lamina a few nanometers thick, which has strong structural similarity to the mammalian nuclear lamina (44). No obvious major lamin bands are detected in the expected 60–70-kDa region by SDS-PAGE (Fig. 5), but if present these components may have altered molecular weights in the trypanosome or be less abundant than in vertebrates. Overall, these data suggest a very high enrichment for the nuclear pore complex and nuclear lamina had been achieved.

Sequence Analysis of Selected Trypanosome Nuclear Proteins—We wished to evaluate the suitability of the nuclear preparations for proteomic analysis. On account of identification of NUP-1 as a relatively abundant Coomassie-stained doublet band coenriching with the NE and PCLF by SDS-PAGE analysis, and the punctate nuclear rim distribution of the antigen under immunofluorescence microscopy (10), we chose this protein for direct proteomic identification of nuclear components. We also excised two of the putative histone bands (Fig. 1), predicted to be trypanosome histone H2B and H4 (32).

We obtained high quality sequence from the H4 and H2B regions that corresponded exactly to trypanosome histone H4 and H2B (Fig. 9A). These proteins, together with the homologues of histones H2A and H3, have previously been characterized at the protein level (32) and confirmed the suitability of our nuclear preparation for proteomics. From the 350-kDa band, we identified a total of five peptides. The first sequence was totally homologous to the \sim 320-kDa microtubule-associated repetitive protein (45), which is localized to the subpellicular microtubule array. Detection of microtubule-associated repetitive protein is probably due to its high abundance in trypanosomes, a repetitive structure (leading to increased stoichiometric representation of the sampled sequence), and a limited association of microtubules with the nucleus.

The remaining four peptides retrieved the same GSS from the Sanger Center data base. Three peptides, ELHVTK, TQLEETV, and LNAAGVR, precisely matched and the fourth, TEEELRTA, was an 89% match. Further data base interro-

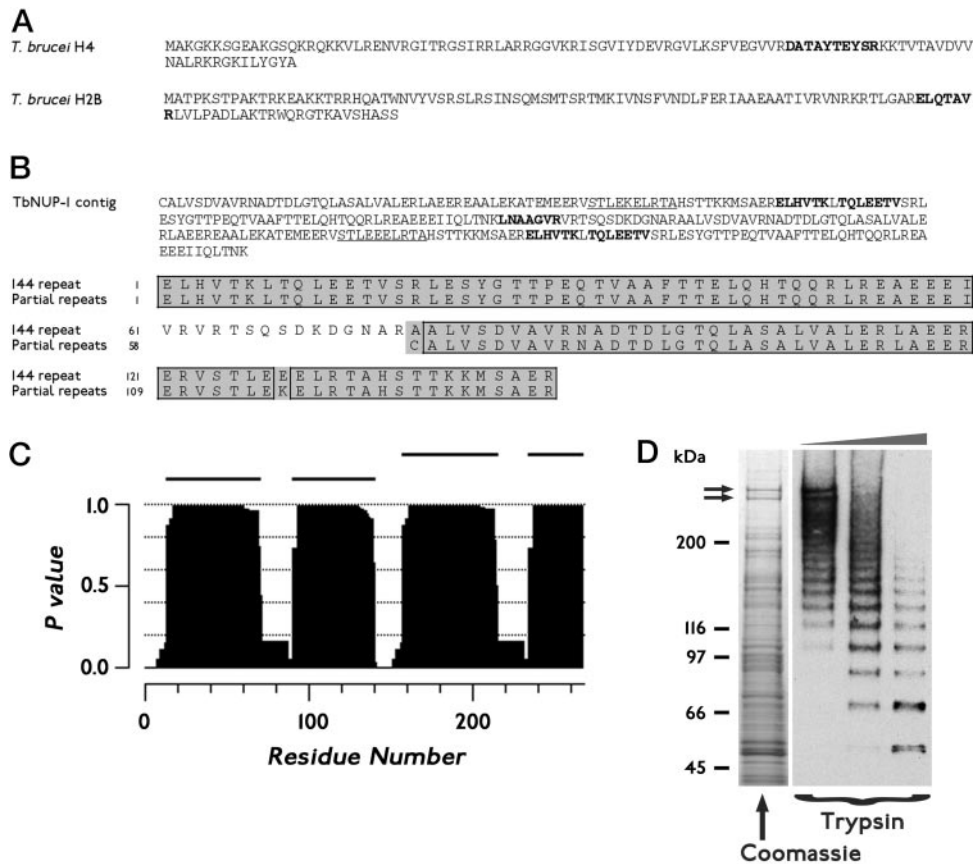


FIG. 9. Identification of the 350-kDa band as the NUP-1 antigen. *A*, protein sequencing data for histone H4 and H2B. Panel shows complete sequences of trypanosome histones H4 and H2B, with the sequences identified by peptide sequencing in *bold*. The molecular sizes of the bands taken for sequencing are consistent with the migration positions of histone H4 and H2B on SDS gels (32). *B*, partial open reading frame assembled from data base retrieved GSSs using four peptide sequences obtained from the 350-kDa band from the NE preparation predicts a coiled coil protein containing 144 amino acid repeats of unmodified molecular mass of 15.9 kDa. Peptides with an exact match are in *bold*, and sequences with a partial match are *underlined*. Alignment of a complete repeat with partial repeat sequences derived from the NH₂ and COOH termini of the assembly reveals an almost perfect repeat structure. The *gap* in the alignment (residues 61–75) represents missing data. *C*, p350 is a coiled coil protein. Secondary structure prediction was done with the Lupas algorithm (27) using MacStripe 2.0a1 with default settings. Two high probability peaks are contained within each repeat. *D*, mild trypsin digestion of isolated nuclei reveals that NUP-1 is a repetitive protein. Digests were analyzed by SDS-PAGE and Western blotting with the NUP-1 antibody. Trypsin treatment reveals a ladder of NUP-1 immunoreactivity, with an approximate repeat mass of 17 kDa, consistent with the repeat identified by peptide sequencing. Increased trypsin digestion results in a greater yield of lower molecular mass products, and indicates that there are ~20 repeats in the NUP-1 protein. Migration positions of molecular size markers are indicated at *left* in kDa.

gation allowed construction of a partial open reading frame of 268 amino acids (Fig. 9*B*). The translated sequence contained a 144-amino acid near-perfect repeat (>98.5% identical), and is strongly predicted to adopt a coiled-coil structure (Fig. 9*C*). The coil frame apparently breaks between each repeat, perhaps indicating an intervening flexible region or turn. As the final assembly produced sequence from three repeats, the incomplete homology of the TEEELRTA peptide can be attributed to repeat microheterogeneity as the related sequences TLEELRTA and TLEELVTA were predicted in the partial open reading frame (Fig. 9*B*).

To confirm that the repetitive 350-kDa protein and the NUP-1 antigen are the same molecule, we subjected isolated NEs to mild trypsin digestion and probed them with the NUP-1 antibody. Trypsinization resulted in cleavage of the NUP-1 antigen into a regular ladder of fragments, with an average separation between products of ~17 kDa, consistent with a single cleavage within the repeat unit of 144 amino acids and confirming the identity between NUP-1 and the sequence retrieved from the data base. At least 20 such repeats were detected in the NUP-1 protein, which accounts for the majority of the molecular mass of the 350-kDa protein (Fig. 9*D*). It is not clear why NUP-1 runs as a doublet, but this may be due to expansion/contraction of the number of repeats through recom-

ination, resulting in different sized gene products expressed either from multiple copies or alleles; a complete explanation must await the full sequence. The assembled portion of the NUP-1 sequence has no specific homologues in the nonredundant data base, but has low homology to a wide variety of proteins with predicted coiled coil structure.

The structure of the NUP-1 antigen suggests that the protein is likely to be a structural nuclear element, and could be a nucleoporin, be part of the nuclear lamina, or have another role. The function of the NUP-1 antigen was further investigated by immunoelectron microscopy (Fig. 10). NUP-1 localizes to the interior face of the NE, ruling it out as a component of the NPC. Rather, this location is consistent with a role for NUP-1 in the nuclear lamina, possibly involved in the organization of the abundant trypanosome perinuclear heterochromatin (Fig. 3). As a major lamina component, and a coiled coil protein, NUP-1 may be a trypanosome orthologue of metazoan lamins. If so, the structure of lamins (which in metazoans generally range in size from only 50 to 70 kDa) is more diverse than previously believed as trypanosomal prenylproteins with a molecular weight similar to metazoan lamins have been detected (46).

The clear presence of a lamina described here has important functional implications. In metazoans, whose nuclei disassem-

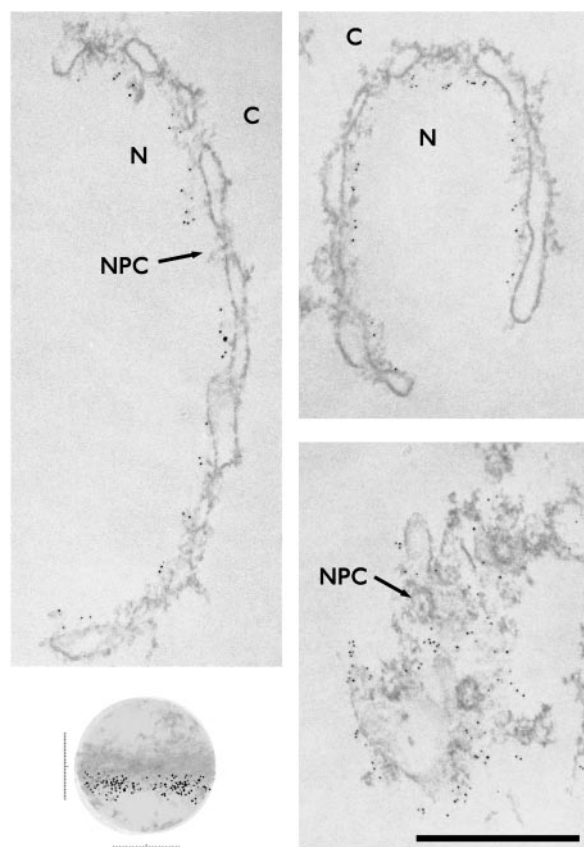


FIG. 10. Immunoelectron microscopy localizes the NUP-1 antigen to the nucleoplasmic face of the nuclear envelope. NEs were incubated with monoclonal antibody NUP-1 and the antibody visualized with gold-conjugated secondary antibodies. *Top left and top right panels*, transverse sections of NEs (C, cytoplasmic side; N, nucleoplasmic side). *Bottom right panel*, tangential section of NE. Scale bar = 0.5 μm . *Bottom left panel*, montage of 40 aligned NPCs showing a total of 198 gold particles. The gold particles are found an average of 57 ± 18 nm from the mid-plane of the NE. Scale bars are graduated in 10-nm intervals. Both the transverse sections and montage indicate that the NUP-1 antigen is localized to a layer beneath the inner face of the NE and that the labeling avoids the vicinity of the NPC.

ble at mitosis, the lamina is believed to play a major role in reformation of the NE during late telophase (47). Thus, yeast, which do not disassemble their NEs at mitosis, lack a lamina (24, 48). However, the presence of a trypanosomal nuclear lamina, which like yeast maintain their nuclear envelopes during mitosis, indicates that the lamina must fulfill a function other than postmitotic NE reformation in these organisms.

CONCLUSIONS

Availability of sequence data bases for an increasing number of divergent eukaryotes represents an excellent opportunity for more rigorous understanding of the repertoire of cellular processes and the degree of variation displayed by these organisms. In particular, this concept justifies much work into pathogenic eukaryotes as a route to development of new chemotherapeutics and other control strategies (e.g. Ref. 4). This extreme divergence also presents a major technical challenge, as identification of function based on homology is frequently not possible. Hence, there is a significant requirement for more direct empirical evidence of function. One strategy is assignment of proteins to specific organelles by direct identification. Our evidence, based on the failure of both *in silico* and immunological similarity, indicates that such approaches are likely to be a vital aspect of postgenomic analysis for many divergent systems.

We chose the trypanosome nucleus for initial entry into

protozoan proteomics for several reasons. First, there is an advanced genome project, facilitating identification of proteins from short peptide sequence. Second, the organism is amenable to study as it can be cultured and there are a number of markers available for the trypanosome nucleus. Third, trypanosomes represent a major global health problem. In a broader context, we also wished to determine if the *T. brucei* nucleus could be used as a test system for establishment of proteomic approaches for other divergent eukaryotes.

Subcellular fractionation of trypanosomatids has been performed by many authors (e.g. Refs. 36 and 49–51), but full morphological and compositional characterization are not available. Our purified nuclear fractions meet several important criteria for proteomic analysis. There is excellent morphological preservation evidenced by EM. The preparations are of high purity, demonstrated by coenrichment of nuclear proteins, EM, and removal of non-nuclear proteins, and are in good yield, as judged from quantitation of nuclear antigens in each fraction. The procedures are scalable (10^{10} to 10^{12} cells may be processed), use standard equipment facilitating exploitation by any laboratory, and can be completed within a day. Hence, it is now possible to progress from trypanosome cultures to a highly enriched nuclear subfraction within 2 days.

The fractionation procedures enabled the identification of the NUP-1 antigen as a repetitive protein, localized to the inner face of the NE, and a probable component of the trypanosome nuclear lamina. Further characterization of NUP-1 function requires further analysis, but characterization of the NUP-1 protein as a major lamina component is an excellent example of the potential of organellar proteomics in divergent systems. Specifically, it is unlikely that the NUP-1 protein could have been identified by interrogation of sequence data bases. Mass spectrometric methods, in combination with one- or two-dimensional gel electrophoresis and other protein separation methodologies may now be used to identify the components of the trypanosome nucleolus, NE and NPC, and distinguish those proteins with expression specific to the PCF or BSF life stages. It is hoped that the methods presented here can be extended, both to isolate other organelles of particular interest from trypanosomes and to isolate subnuclear fractions from other divergent eukaryotes of economic and public health importance. Such methods provide a vital link between genome sequencing projects and functional proteomic applications.

Acknowledgments—We thank the many people who generously provided reagents and advice for this work. Specifically, we thank Caterina Strambio-de-Castillia (Rockefeller University (RU), New York, NY) for monoclonal antibodies against yeast nuclear proteins, Jay Bangs (University of Wisconsin, Madison, WI) for antibodies to TbBiP and p67, Keith Gull and Klaus Ersfeld (University of Manchester, Manchester, United Kingdom) for antibodies against trypanosome tubulin, NUP-1 and NUMAG, and John Boothroyd (Stanford, CA) for anti-RRM1 antisera. We thank George Cross (RU) for bloodstream trypanosome cultures, Günter Blobel (RU) for tissue culture facilities, and Ivan Karnachov (RU) for rat nuclei. We thank Tari Suprpto for help with immunoelectron microscopy, Elena Spicas and Helen Shio for excellent electron microscopy, Rosemary Williams for much superb technical assistance, and Joe Fernandez and Brian Imai for peptide sequencing. We are grateful to the members of the Rout laboratory for (unwittingly, or otherwise) providing many reagents, and much other help. We also thank the following for comments and criticism of the manuscript: Debbie (Biological Sciences, Imperial College, London, UK), Helen Imogen Field (ProteoMetrics LLC, London, UK), and Mark Carrington (Cambridge). We are deeply indebted to Edward Tuft (Harvard University, Cambridge, MA) for insights into data presentation. After submission of this article, the full length ORF for the NUP-1 antigen has been released to GenBank by Dr. Najib El Sayed and colleagues at TIGR. The protein has 18 full repeats, a molecular mass of 406 kDa and is present on *T. brucei* Chromosome II.

REFERENCES

1. Gerhart, J., and Kirschner, M. (1997) *Cells, Embryos, and Evolution*, Blackwell Science, Inc., New York
2. Leadbeater, B. S. C., and Green, J. C. (eds) (2000) *The Flagellates: Unity, Diversity and Evolution*, Taylor and Francis, London
3. Coombes, G. H., Vickerman, K., Sleigh, M. A., and Warren, A. (1998) (eds) *Evolutionary Relationships among Protozoa*, Kluwer Academic Publishers, Dordrecht, The Netherlands
4. Ferguson, M. A. (2000) *Proc. Natl. Acad. Sci. U. S. A.* **97**, 10673–10675
5. Bastin, P., Ellis, K., Kohl, L., and Gull, K. (2000) *J. Cell Sci.* **113**, 3321–3328
6. Wang, Z., Morris, J. C., Drew, M. E., Englund, P. T. (2000) *J. Biol. Chem.* **275**, 40174–40179
7. Pays, E., Vanhamme, L., and Berberof, M. (1994) *Annu. Rev. Microbiol.* **48**, 25–52
8. Bender, K., Betschart, B., Marion, C., Michalon, P., and Hecker, H. (1992) *Acta Trop.* **52**, 69–78
9. Navarro, M., Cross, G. A., and Wirtz, E. (1999) *EMBO J.* **18**, 2265–2272
10. Ogbadoyi, E., Ersfeld, K., Robinson, D., Sherwin, T., and Gull, K. (2000) *Chromosoma* **108**, 501–513
11. Ersfeld, K., Melville, S. E., and Gull, K. (1999) *Parasitol. Today* **15**, 58–63
12. Cross, G. A. (1996) *Bioessays* **18**, 283–291
13. Navarro, M., Ersfeld, K., and Gull, K. (2000) *Molecular Parasitology Meeting, Woods Hole, MA*, p. 18 (abstr.)
14. Rout, M. P., and Aitchison, J. D. (2000) *Essays Biochem.* **36**, 79–85
15. Brun, R., and Schonenberger, S. (1979) *Acta Trop.* **36**, 289–292
16. Field, M. C., and Menon, A. K. (1992) in *Lipid Modifications of Proteins: A Practical Approach* (Hooper, N., and Turner, A. J., eds) pp. 155–190, IRL Press, Oxford
17. Rout, M. P., and Kilmartin, J. V. (1990) *J. Cell Biol.* **111**, 1913–1927
18. Harlow, E., and Lane, D. (1988) *Antibodies: A Laboratory Manual*, Cold Spring Harbor Laboratory Press, Cold Spring Harbor, NY
19. Manger, I. D., and Boothroyd, J. C. (1998) *Mol. Biochem. Parasitol.* **97**, 1–11
20. Field, H., Ali, B. R., Sherwin, T., Gull, K., Croft, S. L., and Field, M. C. (1999) *J. Cell Sci.* **112**, 147–156
21. Field, H., Sherwin, T., Smith, A. C., Gull, K., and Field, M. C. (2000) *Mol. Biochem. Parasitol.* **106**, 21–35
22. Rout, M. P., and Kilmartin, J. V. (1994) in *Cell Biology: A Laboratory Handbook* (Celis, J. E., ed) Vol. 1, pp. 605–612, Academic Press, San Diego
23. Rout, M. P., and Kilmartin, J. V. (1998) in *Cell Biology: A Laboratory Handbook* (Celis, J. E., ed) Vol. 2, pp. 120–128, Academic Press, San Diego
24. Strambio-de-Castillia, C., Blobel, G., and Rout, M. P. (1995) *J. Cell Biol.* **131**, 19–31
25. Kraemer, D. M., et al. (1995) *J. Biol. Chem.* **270**, 19017–19021
26. Rout, M. P., Aitchison, J. D., Suprpto, A., Hjertaas, K., Zhao, Y., and Chait, B. T. (2000) *J. Cell Biol.* **148**, 635–651
27. Lupas, A., Van Dyke, M., and Stock, J. (1991) *Science* **252**, 1162–1164
28. Fernandez, J., Andrews, L., and Mische, S. M. (1994) *Anal. Biochem.* **218**, 112–117
29. Ryan, K. J., and Wente, S. R. (2000) *Curr. Opin. Cell Biol.* **12**, 361–371
30. Field, H., et al. (1994) *Mol. Biochem. Parasitol.* **69**, 131–134
31. Wigge, P. A., Jensen, O. N., Holmes, S., Souès, S., Mann, M., and Kilmartin, J. V. (1998) *J. Cell Biol.* **141**, 967–977
32. Bender, K., Betshardt, B., Schaller, J., Kampf, U., and Hecker, H. (1992) *Parasitol.* **105**, 97–104
33. Bangs, J. D., Andrews, N. W., Hart, G. W., and Englund, P. T. (1986) *J. Cell Biol.* **103**, 255–263
34. Bangs, J. D., Uyetake, L., Brickman, M. J., Balber, A. E., and Boothroyd, J. C. (1993) *J. Cell Sci.* **105**, 1101–1113
35. Fawcett, D. W. (1966) *Am. J. Anat.* **119**, 129–145
36. Shapiro, S. Z., and Doxsey, S. J. (1982) *Anal. Biochem.* **127**, 112–115
37. Hecker, H., Bender, K., Betshardt, B., and Modespacher, U. (1989) *Mol. Biochem. Parasitol.* **37**, 225–234
38. Belli, S. I. (2000) *Int. J. Parasitol.* **30**, 679–687
39. Franke, W. W. (1974) *Int. Rev. Cytol. Suppl.* **4**, 72–236
40. Fountoura, B. M., Blobal, G., Matunis, M. J., et al. (1999) *J. Cell Biol.* **144**, 1097–1112
41. Muramatsu, M., and Onishi, T. (1978) *Methods Cell Biol.* **17**, 141–161
42. Rout, M. P., and Strambio-de-Castillia, C. (1998) *Cell Biology: A Laboratory Handbook*, 2nd Ed., Vol. 2, pp. 143–152, Academic Press, San Diego
43. Rout, M. P., and Aitchison, J. D. (2001) *J. Biol. Chem.* **276**, 16593–16596
44. Dwyer, N., and Blobel, G. (1976) *J. Cell Biol.* **70**, 581–591
45. Afoller, M., Hemphill, A., Roditi, I., Muller, N., and Seebeck, T. (1994) *J. Struct. Biol.* **112**, 241–251
46. Field, H., Blench, I., Croft, S., and Field, M. C. (1996) *Mol. Biochem. Parasitol.* **82**, 67–80
47. Gant, T. M., and Wilson, K. L. (1997) *Annu. Rev. Cell Dev. Biol.* **13**, 669–695
48. Strambio-de-Castillia, C., et al. (1999) *J. Cell Biol.* **144**, 839–850
49. Grab, D. J., Webster, P., Ito, S., Fish, W. R., Verjee, Y., and Lonsdale-Eccles, J. D. *J. Cell Biol.* **105**, 737–746
50. Prado-Figueroa, M., Raper, J., and Opperdoes, F. R. (1994) *Mol. Biochem. Parasitol.* **63**, 255–264
51. Ilgoutz, S. C., Mullin, K. A., Southwell, B. R., and McConville, M. J. (1999) *EMBO J.* **18**, 3643–3654